

Micro Elastic Pouch Motors: Elastically Deformable and Miniaturized Soft Actuators Using Liquid-to-Gas Phase Change

Seiya Hirai, Tatsuho Nagatomo, Takefumi Hiraki , Hiroki Ishizuka, Yoshihiro Kawahara , and Norihisa Miki

Abstract—In the present study, we propose a largely deformable and miniaturized soft actuator that is made by an elastic rubber bladder (called a pouch) with a low-boiling-point liquid. When the temperature of the low-boiling-point liquid reaches 34 °C, the liquid inside the pouch evaporates, and the whole structure inflates. Thanks to the proposed fabrication method, we can make a miniaturized pouch of approximately 5 mm in diameter with a thin rubber membrane, and the pouch can inflate to a volume of 86 times or more compared to its initial volume and can generate approximately 20 N at maximum. We calculated the deformation model and developed the fabrication process through investigation of the thickness and the inflation volume of the pouch with respect to the process parameters. We then experimentally characterized the actuator with respect to the generated force, time response, and repeatability of the inflation. We believe that micro elastic pouch motors will contribute to soft robotic systems as a new component as a result of having unique characteristics, such as millimeter size and large deformability.

Index Terms—Soft sensors and actuators, soft robot materials and design, hydraulic/pneumatic actuators.

I. INTRODUCTION

SOFT robots have been studied to make the best use of their high affinity and safety for a human under daily, typical, and unpredictable environments [1], [2]. Exploration of novel, compliant, and flexible actuators is essential to developing soft robots [3], [4].

Manuscript received October 23, 2020; accepted January 9, 2021. Date of publication April 22, 2021; date of current version May 10, 2021. This letter was recommended for publication by Associate Editor H. Rodrigue and Editor C. Laschi upon evaluation of the reviewers' comments. This work was supported by JST ERATO Grant JPMJER1501, JST CREST Grants JPMJCR19A2, and JSPS KAKENHI Grant JP19J00101, JP20H02121 and JP20K19847. (Corresponding author: Takefumi Hiraki.)

Seiya Hirai, Tatsuho Nagatomo, and Norihisa Miki are with the Graduate School of Science and Technology, Keio University, Kanagawa 223-8522, Japan (e-mail: seiya_hirai@keio.jp; tatsuho19950307@keio.jp; miki@mech.keio.ac.jp).

Takefumi Hiraki is with the Faculty of Library, Information and Media Science, University of Tsukuba, Ibaraki 305-8550, Japan, and also with the Graduate School of Engineering, The University of Tokyo, Tokyo 113-8656, Japan (e-mail: hiraki@slis.tsukuba.ac.jp).

Hiroki Ishizuka is with the Graduate School of Engineering Science, Osaka University, Osaka 305-8550, Japan (e-mail: ishizuka@bpe.es.osaka-u.ac.jp).

Yoshihiro Kawahara is with the Graduate School of Engineering, The University of Tokyo, Tokyo 113-8656, Japan (e-mail: kawahara@akg.t.u-tokyo.ac.jp).
Digital Object Identifier 10.1109/LRA.2021.3075102

Among others, planar pneumatic actuators, such as Peano actuators [5] and pouch motors [6], [7], are considered to have advantages for practical applications. Such advantages include thinness, lightweight, and flexibility, as well as a relatively high power density. These actuators comprise bladders made of elastomers, which are inflated by compressed air supplied via air tubes. However, such pneumatically driven planar actuators are inevitably tethered to bulky and heavy air tubes, valves, and pumps, which spoils the soft, lightweight, and flexible characteristics of these actuators.

In order to address this problem, HASEL actuators [8]–[10] and liquid-to-gas phase-change actuators [11]–[15] have been proposed, and these actuators encapsulate a functional fluid inside the bladder and use the intrinsic characteristics of the liquid. Since these actuators are free from the pneumatic tubes, valves, and large air compressors needed to drive the actuator, the systems can be simplified and are more highly suitable for soft robots. In particular, liquid-to-gas phase-change actuators do not require a high voltage of more than 1 kV, which is required by HASEL actuators. On the other hand, although the volume increases more than a thousand-fold in the phase change from liquid to gas, these liquid-to-gas phase-change actuators cannot fully exploit this increase because their bladders are stiff and cannot expand. Altmüller *et al.* [16] proposed a liquid-to-gas phase-change actuator with soft dielectric membranes. However, the expansion rate of the actuator remained at only 1.2 times.

Soft actuators that contain sub-millimeter ethanol liquid droplets inside a silicone elastomer [17] and deionized water inside a carbon fiber sleeve [18] have been proposed. By exploiting the liquid-to-gas phase change of the liquid, the actuators were successfully installed in soft robots. The challenges are that the actuators are soft, yet not stretchable, and the expanded volume was 10 times their initial volume at maximum. In addition, miniaturization may be difficult due to the complexity of the structure.

Accordingly, the size of a bladder must be enlarged to achieve a sufficient deformation. Therefore, thus far, miniaturization of the actuators has not been investigated, let alone the fabrication processes.

In the present letter, we propose the micro elastic pouch motor (mEPM), which is an elastically deformable spherical-shaped

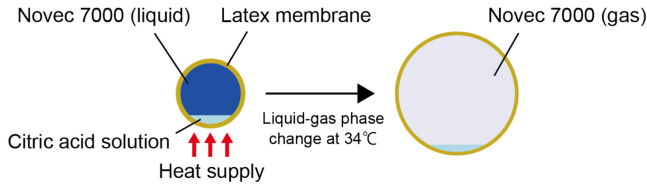


Fig. 1. Structure and principle of the micro elastic pouch motor (mEPM), which is an elastically deformable and miniaturized liquid-to-gas phase-change soft actuator. The actuator is composed of a thin latex pouch with a low-boiling-point liquid (Novec 7000, 3 M Company), which evaporates at 34° . The citric acid solution in the pouch is used for the fabrication and does not affect the expansion.

millimeter-sized fluidic actuator that exploits the phase change of a low-boiling-point liquid, Novec 7000 (3 M Company). The boiling point of the liquid is as low as 34° . Note also that the liquid has good biocompatibility and is not flammable. We developed an encapsulating process of a low-boiling-point liquid with an elastic rubber membrane to form a millimeter-scale sphere, which does not include any heating processes. Fig. 1 shows the structure and principle of the mEPM. Owing to its structure and material, the spherical rubber pouch could be miniaturized to 5 mm in diameter and can inflate greatly, as compared with conventional actuators containing low-boiling-point liquid Novec 7000 [11]–[15], [19]. The proposed actuator that can generate a significant force (max. 20 N).

The contributions of the present letter can be summarized as follows:

- The concept of a novel elastically deformable and miniaturized soft actuator is proposed, and the theoretical deformation is estimated.
- The fabrication process of the proposed actuator is developed, and the thickness and the inflation volume of the elastic pouch with respect to the fabrication parameters are investigated.
- The performance of the proposed actuator is assessed through three experiments. These experiments reveal that the actuator can generate a force of 20 N at maximum and a stress of 0.12 MPa, while the proposed actuator can expand up to 86 times its original size.

II. MICRO ELASTIC POUCH MOTORS (MEPMS)

A. Overview

Micro elastic pouch motors (mEPMS) have spherical pouches made of elastic rubber in which the low-boiling-point liquid is encapsulated. We selected a hydrofluoroether (Novec 7000, 3 M Company) as the low-boiling-point liquid because it is non-flammable and safe for humans and the environment. It has been reported that many kinds of elastic polymers, such as widely used polydimethyl-siloxane (PDMS), are permeable with respect to Novec 7000 [20]. We selected latex rubber as the elastic material to compose the pouch because latex rubber rarely absorbs Novec 7000 [21].

We fabricated latex rubber pouches using the flocculation reaction of a latex suspension and a citric acid aqueous solution. This reaction progresses immediately, and Novec 7000 can be encapsulated without evaporation at room temperature. Thanks

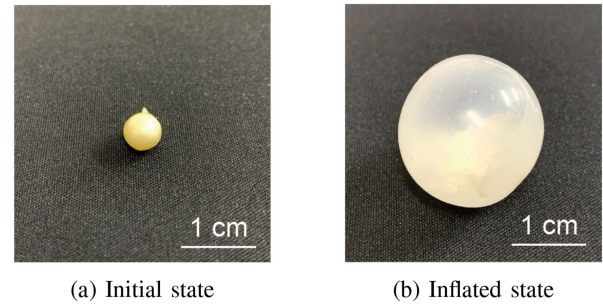


Fig. 2. Actuation of the micro elastic pouch motor (mEPM). (a) The pouch of the actuator is 5 mm in diameter in the initial state. (b) In this figure, the mEPM is expanded to approximately 86 times its initial volume when the surface temperature reaches 60° .

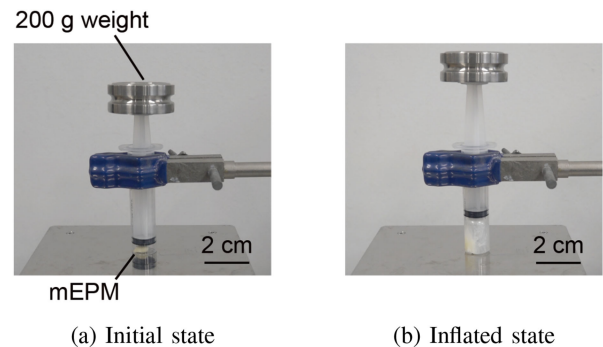


Fig. 3. Linear motion structure with an mEPM. The piston structure converts the inflation of the mEPM into linear motion that is sufficient to lift a weight (200 g).

to the low elastic modulus of latex rubber, the actuator can be inflated greatly and spherically with the liquid-to-gas phase change. Thus, the actuator can generate a large displacement and force considering its size (on the order of millimeters).

Fig. 2 shows an mEPM in an initial state and an inflated state. The developed process enables us to create an elastically deformable actuator with a miniaturized pouch of 5 mm in diameter. This actuator can expand 86 times its initial volume, which is significantly larger than the expansion rate of the previous elastically deformable liquid-to-gas phase-change actuator [16].

Thanks to the miniaturized and largely deformable nature of the mEPM, we can easily apply the actuator to soft robots that deform in various ways. Fig. 3 shows the linear motion structure of the mEPM. We embedded the mEPM in a chamber in the piston structure and inflated the mEPM by heating, thereby successfully realizing linear up-and-down motion. This motion is sufficient to lift a weight (200 g). Fig. 4 shows the angular motion possible with multiple mEPMS. We fixed mEPMS on a PDMS substrate (Silpot 184 W/C, Dow Corning Toray Co., Ltd.) at even intervals, using its ease of arraying. The structure stands upright in the initial state. The mEPMS pressed against each other, and the end-to-end length of the mEPMS increased in the inflated state. The difference between this end-to-end length and the PDMS substrate length results in bending of the structure.

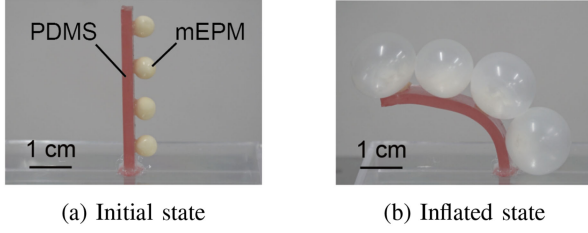


Fig. 4. Angular motion structure with an mEPM. (a) The structure stands upright in the initial state. (b) The difference between the strains on the right-hand side and the left-hand side of the structure occurred in the inflated state. This results in bending of the structure.

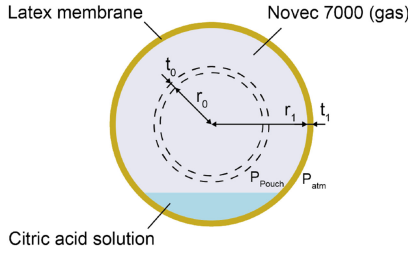


Fig. 5. Deformation model of the pouch of an mEPM. Here, P_{Pouch} is the pressure inside the pouch, and P_{atm} is atmospheric pressure. Moreover, t_0 and t_1 are the thicknesses of the membrane in the initial state and the inflated state, respectively, and r_0 and r_1 are the radiuses of the pouch in the initial state and the inflated state, respectively.

B. Deformation Model

Here, we model the pouch structure of the mEPM and deduce the relationship between the pressure and the size of the pouch. Fig. 5 illustrates the theoretical deformation model of the pouch and its parameters. In the model, the pouch is considered to always be spherical. The deformation of the pouch is induced by the inside pressure. With the Young-Laplace equation, the pressure difference between the inside and the outside (atmospheric pressure) can be expressed as follows:

$$P_{Pouch} - P_{atm} = \frac{2\sigma t_1}{r_1} \quad (1)$$

where P_{Pouch} [kPa] is the pressure inside the pouch, P_{atm} [kPa] is the atmospheric pressure, t_1 [mm] is the thickness of the rubber membrane in the inflated state, r_1 [mm] is the radius of the pouch, and σ [kPa] is the tensile stress on the membrane. In the spherical coordinate system, the relationship between the stress and the strain of the membrane can be expressed as follows:

$$\epsilon_\theta = \frac{1}{E}(\sigma_\theta - \nu\sigma_\phi) \quad (2)$$

$$\epsilon_\phi = \frac{1}{E}(\sigma_\phi - \nu\sigma_\theta) \quad (3)$$

where σ_θ [kPa] and σ_ϕ [kPa] are the stress at the zenith and azimuth angles, respectively, ϵ_θ and ϵ_ϕ are the strain at the zenith and azimuth angles, respectively, and E [kPa] and ν are Young's modulus and Poisson's ratio of latex rubber, respectively. When we hypothesize the isotropic stress and strain, (2) and (3) can be

modified as follows:

$$\sigma = \frac{E}{1-\nu}\epsilon \quad (4)$$

where ϵ is the strain of the membrane.

The strain can be expressed as the change in the diameter. Here, ϵ is derived as follows:

$$\epsilon = \frac{2\pi r_1 - 2\pi r_0}{2\pi r_0} = \frac{r_1 - r_0}{r_0} \quad (5)$$

where r_0 is the initial radius of the pouch. Assuming that the volume of the membrane is always constant, the following equation is obtained:

$$4\pi r_1^2 t_1 = 4\pi r_0^2 t_0 \quad (6)$$

where t_0 [mm] is the thickness of the membrane in the initial state. By simplifying this equation, t_1 can be expressed as follows:

$$t_1 = \frac{r_0^2}{r_1^2} t_0 \quad (7)$$

From (13), (4), (5), and (7), the following equation is obtained:

$$P_{Pouch} - P_{atm} = \frac{2Er_0 t_0}{1-\nu} \frac{r_1 - r_0}{r_1^3}. \quad (8)$$

When the pressure of Novoc 7000 P_{Novoc} [kPa] is given, P_{Novoc} is derived using the state equation $PV = nRT$ as

$$P_{Novoc} = \frac{1}{V_{Pouch}} \frac{V_{Novoc} \rho}{M} RT \quad (9)$$

where V_{Pouch} [mm³] is the volume of the inflated pouch, V_{Novoc} [mL] is the injected volume of Novoc 7000, ρ [gmL⁻¹] is the density of Novoc 7000, M [gmol⁻¹] is the molar mass of Novoc 7000, R [JK⁻¹ mol⁻¹] is the gas constant, and T [K] is the absolute temperature of Novoc 7000 inside the pouch.

Here, P_{Water} [kPa] is the vapor pressure of the citric acid solution, and P_{Pouch} is obtained as the sum of P_{Novoc} and P_{Water} . Using this relation and (9), P_{Pouch} is calculated as follows:

$$\begin{aligned} P_{Pouch} &= P_{Novoc} + P_{Water} \\ &= \frac{V_{Novoc} \rho RT}{V_{Pouch} M} + P_{Water} \end{aligned} \quad (10)$$

Assuming that the shape of the pouch is always spherical, V_{Pouch} is expressed as follows:

$$V_{Pouch} = \frac{4}{3}\pi r_1^3 \quad (11)$$

Using (8), (10), and (11), the following equation is obtained:

$$\begin{aligned} \frac{P_{Water} - P_{atm}}{2t_0 r_0} r_1^3 - \frac{E}{1-\nu} (r_1 - r_0) \\ + \frac{3}{8} \frac{V_{Novoc} \rho RT}{\pi M t_0 r_0} = 0 \end{aligned} \quad (12)$$

The theoretical size of the spherical pouch can be calculated with the approximate solution of r_1 obtained with (12). Tables I and II show the constant parameters and the calculated volumes, respectively.

TABLE I
VALUES OF THE PARAMETERS FOR THE DEFORMATION MODEL. THE
PARAMETERS FOR NOVEC 7000 ARE DERIVED FROM [21]

Parameter	Description	Value
ρ	Density of Novec™ 7000	1.4 g mL ⁻¹
R	Universal gas constant	8.314 J K ⁻¹ mol ⁻¹
T	Temperature of the environment	333 K
M	Molar mass of Novec™ 7000	200 g mol ⁻¹
t_0	Initial thickness of the bladder	0.6 mm
r_0	Initial radius of the bladder	2 mm
P_{Water}	Vapor pressure of water at T [K]	19.937 kPa
P_{atm}	Atmospheric pressure	101.325 kPa
E	Young's modulus of latex	1500 kPa
ν	Poisson's ratio of latex	0.46

TABLE II
PARAMETERS AND RESULTS OF THE THEORETICAL CALCULATION. HERE,
 V_{Novec} AND W_{Novec} ARE KNOWN, AND V_{Novec} IS CALCULATED USING
THESE TERMS

V_{Novec} [mL]	0.01	0.02	0.03	0.04	0.05
W_{Novec} [g]	0.014	0.028	0.042	0.056	0.07
V_{Pouch} [mm ³]	995	2574	4385	6315	8318

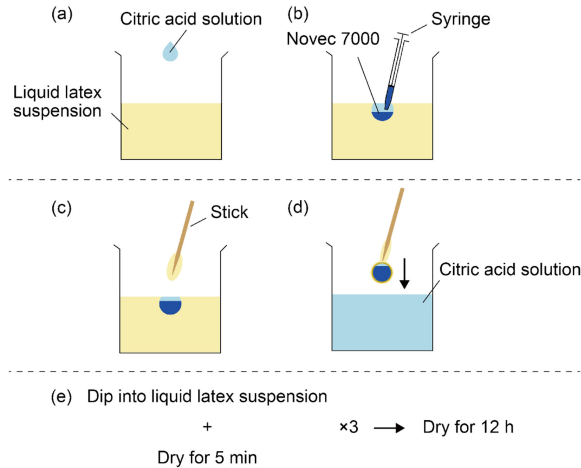


Fig. 6. Fabrication process of the mEPM. (a) Dispense the citric acid solution into the liquid latex suspension. (b) Inject Novec 7000 into the citric acid droplet. (c) Pick up the pouch with a stick. (d) Dip the pouch into the citric acid solution for sufficient coagulation of the latex. (e) Repeatedly, dip the pouch into the liquid latex suspension and dry.

III. FABRICATION PROCESS

A. Overview

Novec 7000 needs to be encapsulated by a membrane that is elastically deformable and nonabsorbent Novec 7000. Therefore, we use latex rubber as a membrane. Note that heat sealing cannot be used as previously proposed [13], [14] given the low boiling point of Novec 7000. We attempted to use the coagulation processes of the latex suspension and the citric acid solution. The spherification process to produce beads by chemical reaction has been proposed [22]. However, the mEPM is the first actuator to encapsulate Novec 7000 in a spherical latex membrane. Fig. 6 shows the fabrication process of the proposed actuator.

The steps of the fabrication process are as follows:

- A volume of 0.02 mL of a citric acid aqueous solution is dispensed into a liquid latex suspension (PC-518,

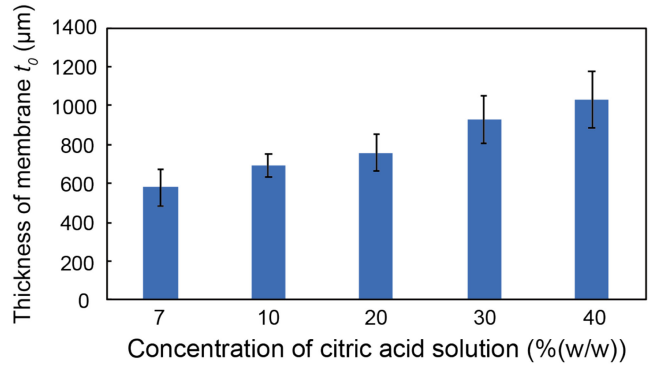


Fig. 7. Relationship between the thickness and the concentration of citric acid. The thickness increases with the concentration.

HR-TEC) in a beaker, which induces the coagulation reaction, and a thin latex membrane is formed at the interface.

- Novec 7000 is directly injected into the citric acid droplet using a 1.0 mL syringe (SS-01 T, TERUMO). The volume of Novec 7000 is varied from 0.01 mL to 0.05 mL.
- After the droplet is covered with the latex suspension, the pouch is picked up with a stick. Novec 7000 is completely encapsulated inside the latex rubber pouches without evaporation.
- The pouch is dipped into the citric acid solution to sufficiently promote the coagulation to form a pouch.
- The pouch is dipped into the liquid latex suspension and its surface is dried for 5 min.
- Step (e) is iterated two more times in order to cover the droplet completely with the latex membrane, which prevents leakage when expanded. Finally, the pouch is dried for 12 hours.

B. Pouch Thickness

We investigated the thickness of the latex rubber pouch, which determines the mechanical properties of the membrane, including stiffness and thermal conductivity. We experimentally investigate the relationship between the thickness and concentration of citric acid. We varied the concentration of the citric acid from 10% (w/w) to 40% (w/w) at intervals of 10% (w/w), where the solubility of the citric acid in water is 7 g/100 ml and the maximum concentration of the dispensable citric acid solution is 42% (w/w).

We fabricated the pouches using the proposed fabrication process. We cut these pouches and measured the membrane thickness using a laser microscope (VK-X 100, KEYENCE). We prepared ten samples for each concentration condition and acquired their average thicknesses. In addition, we investigated the minimal formable thickness of the latex membrane using the fabrication process. We increased the concentration of citric acid from 1% (w/w) at an interval of 1% (w/w) and searched the minimal concentration at which the latex membrane was successfully formed.

The average thickness of the pouch is shown in Fig. 7. The thickness of the latex membrane increased with the concentration of the citric acid. The standard deviation of the thickness was small compared to the thickness. Thus, we conclude that

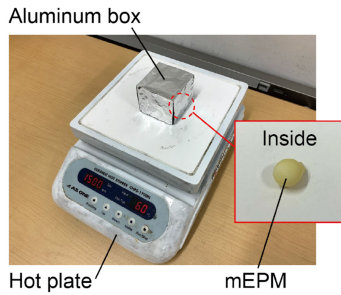


Fig. 8. Experimental setup for the inflation volume measurement. We covered the mEPM with an aluminum box in order to maintain a temperature constant.

the proposed fabrication process has good repeatability. The smallest latex membrane thickness was approximately $600 \mu\text{m}$ when the concentration of the citric acid was 7% (w/w). In the following experiments, we used a 7% (w/w) citric acid solution to form the thinnest latex membrane, expecting the highest deformability and thermal conductivity.

C. Inflation Volume of the Pouch

We investigated the inflation volume of the latex rubber pouch with respect to the volume of encapsulated Novec 7000.

Fig. 8 shows the experimental setup. We placed the latex rubber pouch on a hot plate (CHPS-170DN, AS ONE). We covered the pouch on the hot plate with aluminum foil for efficient and uniform heating. We set the temperature of the hot plate as 60° and heated the pouch for 3 min on the hot plate. Then, we measured the diameter in the triaxial axis by taking pictures of the pouch from three directions and analyzed these images using graphics editing software (Adobe Photoshop CC, Adobe Inc.). We calculated the volume of the pouches ($n = 10$) based on its diameter under the assumption that the pouch was spherical. This assumption comes from the fact that the bond number of the mEPM is smaller than one. The bond number is the dimensionless number that shows the dominance of surface tension and gravity, which is expressed as the ratio of the capillary length to the actual diameter of the droplet, as follows:

$$Bo = \left(\frac{L}{l}\right)^2 \quad (13)$$

where Bo is the bond number, L [mm] is the length of the droplet, and l [mm] is the capillary length of the liquid. If the bond number is smaller than 1, we can say that the surface tension is more dominant than gravity. The diameter of a citric acid solution droplet ($L = 1.68 \text{ mm}$) is smaller than the capillary length of water ($l = 2.7 \text{ mm}$). Thus, it is considered that the droplet can ignore gravity and form a spherical shape. Since the applied pressure of a gas is constant in every direction, the inflated pouch would also have a spherical shape. The injection volume of Novec 7000 from 0.01 mL to 0.05 mL was tested.

Fig. 9 shows the obtained results. We plotted both the measured volume on average and the theoretical volume of the pouches calculated using Eq. (12). The volume of the pouch linearly increased with the injection volume of Novec 7000. The order and trend of the experimental results agreed with the

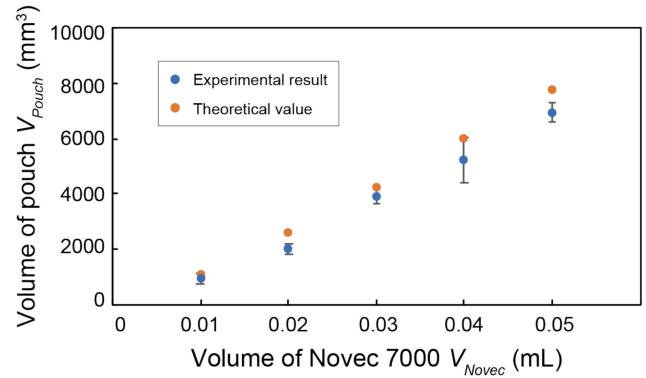


Fig. 9. Relationship between the inflation volume of the pouch and the injection volume of Novec 7000. The inflation volume increases as the injection volume increases.

TABLE III
VOLUME OF THE LATEX RUBBER POUCHES (V_{Pouch}) IN THE NON-INFLATED AND INFLATED STATES. THE VOLUME WAS CALCULATED BASED ON THE MEASURED DIAMETER

V_{Novec} [mL]	0.01	0.02	0.03	0.04	0.05
$r_0 + t_0$ [mm]	2.6				
$r_1 + t_1$ [mm]	6.1	8.4	9.4	10.3	11.5
V_{Pouch} (initial) [mm ³]	73.6				
V_{Pouch} (inflated) [mm ³]	951	2482	3479	4577	6371
Radius ratio	2.35	3.22	3.60	3.95	4.42
Volume ratio	12.9	33.7	47.2	62.2	86.6

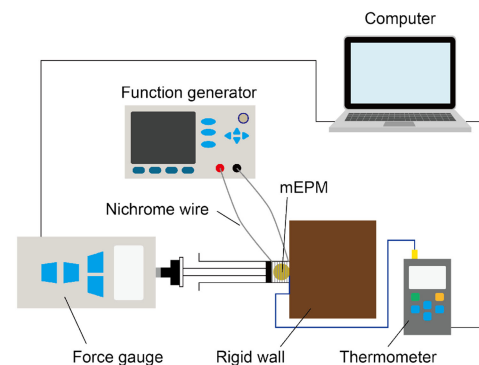


Fig. 10. Experimental setup for force measurement.

theory. The encapsulated citric acid does not affect the expansion, which was verified by the experimental results whereby an mEPM containing only citric acid failed to expand. We summarized the values of the measured diameter and volume in Table III. This table shows that the pouch can inflate to more than 86 times its initial volume, which is larger in magnitude than previous elastically driven actuators [17].

IV. EXPERIMENTS

A. Generated Force of the mEPM

In order to verify the performance as an elastically deformable soft actuator, we investigated the force that an mEPM can produce with respect to the injection volumes of Novec 7000. Fig. 10 illustrates the experimental setup of this measurement. In order to suppress circumferential expansion, we placed the

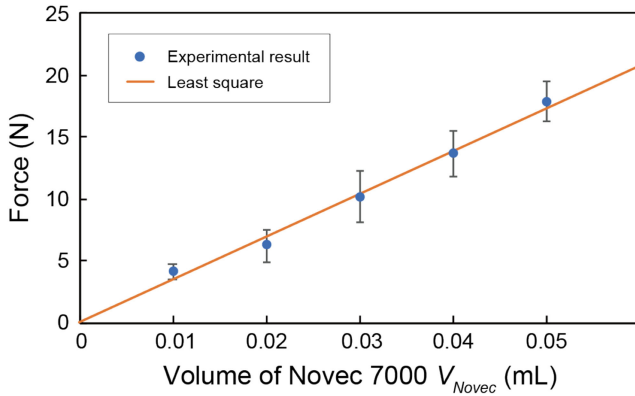


Fig. 11. Relationship between generated force and injection volume of Novec 7000. The force is proportional to the injection volume.

pouch of the mEPM in a syringe (SS-10SZ, TERUMO) with its tip cut off and measured the pushing force of the syringe using a force gauge (DST-500 N, IMADA). We twined a nichrome wire (0.4 mm in diameter) around the syringe and heated the pouch to 60° by applying 0.7 A of DC with an electrical power supply (WF1974, WAVE FACTORY). We measured the temperature of the pouch in the syringe using a thermometer (CENTER 520, CENTER TECHNOLOGY). We prepared actuators fabricated with injection volumes of Novec 7000 from 0.01 mL to 0.05 mL. We tested ten samples for each condition.

Fig. 11 shows the peak output forces of the actuators. The actuator with 0.05 mL of injected Novec 7000 successfully produced an output force of approximately 20 N. The expansion of the mEPM was converted into the linear actuation of the cylinder structure. The friction force induced by the structure is on the order of 1 N, which is negligible compared to the generated force. The relationship between the injection volumes of Novec 7000 and the output forces can be approximated by a line ($R^2 = 0.998$). Based on this relationship, we can obtain a design guideline for the maximum power characteristics of the mEPM.

Under these experimental conditions, P_{Pouch} does not reach the vapor pressure of Novec 7000, and thus all of the Novec 7000 was vaporized. This is verified by the fact that the output force is proportional to the injected volume. However, it can reach saturation when we add a larger amount of Novec 7000 and some remains as a liquid at expansion.

The stress is calculated to be approximately 0.12 MPa by dividing the force by the cross-sectional area of the syringe. This stress is rather small but is competitive with natural muscle and DEA [17]. On the other hand, the proposed mEPM has a unique flexibility.

B. Time Response of the mEPM

In order to investigate the time response of the force generated by an mEPM, we measured the force using the same setup as the experiment in Section IV-A. We conducted the experiment using actuators with injection volumes of Novec 7000 from 0.01 mL to 0.05 mL. In this experiment, we used the force logger software of the force gauge to record the measured force every second.

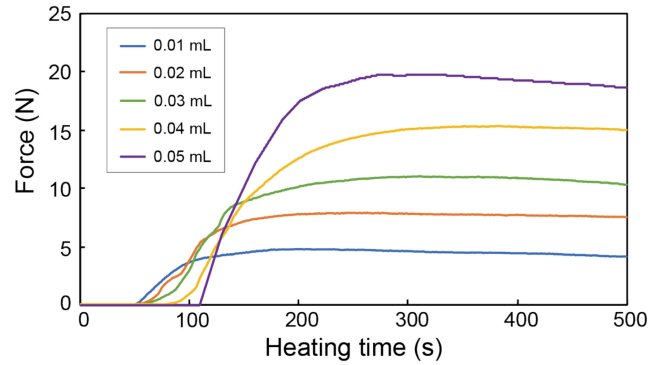


Fig. 12. Relationship between pushing force and heating time. The larger the injection volume, the longer it takes for the force to saturate.

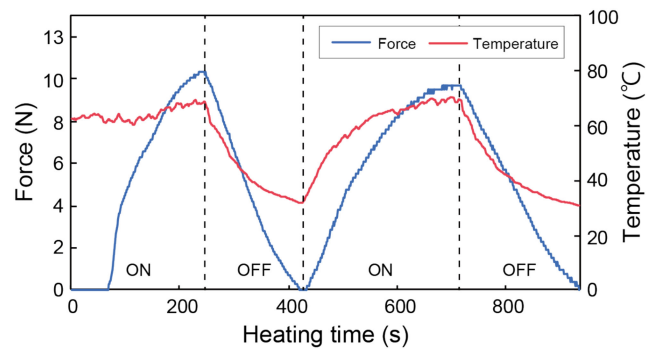


Fig. 13. Response of pushing force and temperature in the cycle test. The pushing force changed with the temperature.

Fig. 12 shows the pushing force with respect to the heating time. As the volume of Novec 7000 injected increased, the start time of inflation became slower. This is because a larger volume of Novec 7000 requires more heat for vaporization due to the higher heat capacity. The rate of decrease in the pushing force after 200 s from the peak force at each Novec 7000 injection volume was calculated to be approximately 5%. This result indicates that an mEPM can maintain the pushing force for a few hundred seconds.

We also investigated the effect of the mEPM temperature on the pushing force using the same setup. We measured the pushing force, the heating time, and the temperature inside the syringe in this experiment. We controlled the temperature inside the syringe at 60° until the pushing force became stable for 5 s. Then, we stopped heating until the pushing force returned to 0 N. We increased the temperature inside the syringe to 60° again and stopped heating when the force became stable for 5 s. We used the actuator with the injected Novec 7000 of 0.03 mL in this experiment.

Fig. 13 shows the experimental results. The pushing force increased in the heating process and decreased in the cooling process. The force dropped to zero when the temperature reached approximately 34° , which is the boiling point of Novec 7000. Interestingly, the peak force in the second heating was smaller than that in the first heating. There is a possibility that Novec 7000 gas permeated through the latex membrane, and the fluid inside

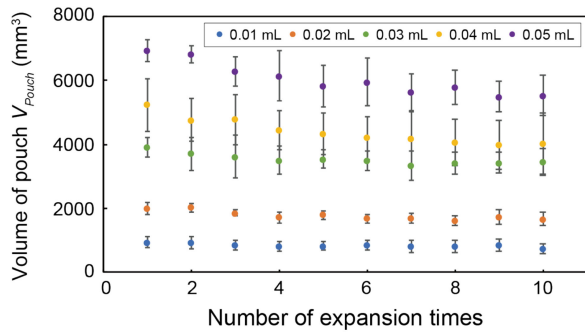


Fig. 14. Volume of the inflated pouch during 10 heating and cooling cycles. The volume decreased with the number of cycles.

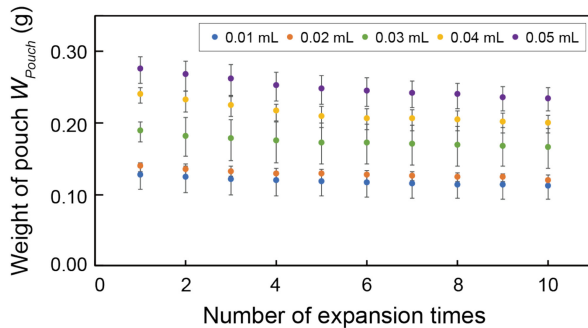


Fig. 15. Weight of the inflated pouch during 10 cycles. The weight decreased with the number of cycles.

the pouch was lost. This result will be discussed in more detail in the following section.

C. Repeatability of the mEPM

In order to observe the reproducibility of the inflation motion of the mEPM, the volume and weight of the pouch were measured during ten heating and cooling cycles. We conducted the experiment with the same experimental setup as that used in Section III-C. We used five mEPMs for each injection volume of Novec 7000 (0.01 mL – 0.05 mL). We heated the pouch to 60° heated the pouch for 3 min on a hot plate and measured the diameter of the triaxial axis using graphic editor software. We also measured the weight using an analytical balance (AUW120D, SHIMADZU). After these measurements, we cooled the pouch at room temperature (19°) for 300 s. These processes were iterated ten times.

Figs. 14 and 15 show the volume and weight of the inflated pouch measured in each cycle, respectively. The results show that both the volume and weight of Novec 7000 were decreased as the cycle was iterated. This indicates that leakage of the Novec 7000 in the gas phase occurred. When the pouch inflates, the latex membrane is stretched, which promotes leakage. This effect is more significant during the first couple of cycles, which was verified by the experimental results. The permeation is unavoidable when elastic materials, which include latex rubber, are in contact with gases. Thus, the effect of the permeation must be considered in the design of the mEPM.

V. DISCUSSION

A. Fabrication Process

This pouch has the advantage of being of millimeter size yet capable of producing a large force. In order to further promote this advantage of miniaturization, microfabrication can be proposed. In the present study, we fixed the volume of Novec 7000 and evaluated the effect of the concentration of the citric acid solution on the thickness of the latex bladder. Miniaturization of citric acid droplets may lead to even smaller pouches. Microdroplet generation has been widely studied in the field of microfluidics [23], [24]. The downsizing will contribute to the quick deformation response of the pouch because of its low heat capacity.

B. Pouch Heating

Although the mEPM is largely deformable and miniaturized, its response time for expansion can still be improved by designing more efficient heating systems. From the experiments in Section IV-B, the mEPM required 50 s–100 s to start inflation when heated in contact with a heater. This response time was slower than that of conventional liquid-to-gas phase change actuators, which starts expanding within approximately 30 s [13], [14]. We assumed that this slow response is caused by the poor thermal conductivity of the pouch due to the material (latex rubber) and the thickness of the membrane. The thickness of the latex rubber membrane (600 μm) is larger than that of conventional actuators (50 μm in [13], [14]).

Exploring more efficient pouch heating methods may alleviate this slow response. Altmüller *et al* [16] and Usui *et al* [25] embedded a heater device inside the pouch, and contact-less heating methods for the liquid-to-gas phase-change actuators using induction heating [19], laser heating [26], [27], and microwaves [28] have also been proposed. These methods can heat the pouches locally and can be less affected by the environment, as compared to heating methods using a hot plate or hot airflow.

C. Leakage of the Low-Boiling-Point Liquid

Through the experiments, the efficiency of the elastic pouch as an actuator was verified. The pouch produced a high pushing force despite the millimeter size. However, there remain limitations in use as an actuator. One of the main concerns is that Novec 7000 leaks out of the nano-sized gaps in the latex membrane during expansion, even though the material absorbs Novec 7000 less than other elastic materials. This can be inferred from the force reduction in the experiments in Section IV-B and the repeatability in the experiment in Section IV-C. The gas of Novec 7000 leaked out of the pouch, particularly when the pouch inflated and the membrane was stretched. The available volume of Novec 7000 gradually decreased with this leakage. In addition, leakage can be suppressed by applying a thin barrier film to the latex membrane. It was reported that appropriate parylene coating reduces the gas permeation via polymers without reducing the elasticity of the latex membrane [29].

VI. CONCLUSION

A micro elastic pouch motor (mEPM) that can exhibit large deformation using the liquid-to-gas phase change is proposed and characterized. A low-boiling-point liquid, Novec 7000 is encapsulated in an elastic latex rubber pouch by means of a coagulation-based fabrication process. In the present letter, we measured the volume of expansion, repeatability, output force, and response speed of the elastic pouch. The experiments verified that the elastic pouch actuator generates a large amount of force of 20 N for a diameter of 5 mm. The proposed mEPM can be readily applied to a wide range of applications as a millimeter-sized, soft, and efficient actuator.

REFERENCES

- [1] M. T. Tolley *et al.*, "A resilient, untethered soft robot," *Soft Robot.*, vol. 1, no. 3, pp. 213–223, Sep. 2014.
- [2] D. Rus and M. T. Tolley, "Design, fabrication and control of soft robots," *Nature*, vol. 521, no. 7553, pp. 467–475, May 2015.
- [3] S. I. Rich, R. J. Wood, and C. Majidi, "Untethered Soft Robotics," *Nature Electron.*, vol. 1, pp. 102–112, Feb. 2018.
- [4] Y. Liu *et al.*, "Epidermal mechano-acoustic sensing electronics for cardiovascular diagnostics and human-machine interfaces," *Sci. Adv.*, vol. 2, no. 11, Nov. 2016, Art. no. e1601185.
- [5] S. Sanan, P. S. Lynn, and S. T. Griffith, "Pneumatic torsional actuators for inflatable robots," *J. Mechanisms Robot.*, vol. 6, no. 3, pp. 031003:1–031003:7, Apr. 2014.
- [6] R. Niiyama, D. Rus, and S. Kim, "Pouch motors: Printable/inflatable soft actuators for robotics," in *Proc. IEEE Int. Conf. Robot. Automat.*, Sep 2014, pp. 6332–6337.
- [7] R. Niiyama, X. Sun, C. Sung, B. An, D. Rus, and S. Kim, "Pouch motors: Printable soft actuators integrated with computational design," *Soft Robot.*, vol. 2, no. 2, pp. 59–70, Jun. 2015.
- [8] E. Acome *et al.*, "Hydraulically amplified self-healing electrostatic actuators with muscle-like performance," *Science*, vol. 359, no. 6371, pp. 61–65, Jan. 2018.
- [9] N. Kellaris, V. G. Venkata, G. M. Smith, S. K. Mitchell, and C. Keplinger, "Peano-HASEL actuators: Muscle-mimetic, electrohydraulic transducers that linearly contract on activation," *Sci. Robot.*, vol. 3, no. 14, Jan. 2018, Art. no. eaar 3276.
- [10] S. K. Mitchell *et al.*, "An easy-to-implement toolkit to create versatile and high-performance HASEL actuators for untethered soft robots," *Adv. Sci.*, vol. 6, no. 14, Jun. 2019, Art. no. 1900178.
- [11] T. Akagi, S. Dohta, S. Fujimoto, Y. Tsuji, and Y. Fujiwara, "Development of flexible thin actuator driven by low boiling point liquid," *Int. J. Mater. Sci. Eng.*, vol. 3, no. 1, pp. 55–59, 2015.
- [12] Y. Tsuji, S. Dohta, T. Akagi, and Y. Fujiwara, "Analysis of flexible thin actuator using gas-liquid phase-change of low boiling point liquid," in *Proc. 3rd Int. Conf. Intell. Technol. Eng. Syst.*, vol. 345, 2016, pp. 67–73.
- [13] K. Nakahara, K. Narumi, R. Niiyama, and Y. Kawahara, "Electric phase-change actuator with inkjet printed flexible circuit for printable and integrated robot prototyping," in *Proc. IEEE Int. Conf. Robot. Automat.*, Jul. 2017, pp. 1856–1863.
- [14] K. Narumi *et al.*, "Liquid pouch motors: Printable planar actuators driven by liquid-to-gas phase change for shape-changing interfaces," *IEEE Robot. Automat. Lett.*, vol. 5, no. 3, pp. 3915–3922, Jul. 2020.
- [15] V. Sanchez *et al.*, "Smart thermally actuating textiles," *Adv. Mater. Technol.*, vol. 5, no. 8, Aug. 2020, Art. no. 2000383.
- [16] R. Altmüller, R. Schwödiauer, R. Kaltseis, S. Bauer, and I. M. Graz, "Large area expansion of a soft dielectric membrane triggered by a liquid gaseous phase change," *Appl. Phys. A: Mater. Sci. Process.*, vol. 105, no. 1, pp. 1–3, Oct. 2011.
- [17] A. Miriyev, K. Stack, and H. Lipson, "Soft material for soft actuators," *Nat. Commun.*, vol. 8, no. 1, pp. 1–8, Sep. 2017.
- [18] S. M. Mirvakili, D. Sim, I. W. Hunter, and R. Langer, "Actuation of untethered pneumatic artificial muscles and soft robots using magnetically induced liquid-to-gas phase transitions," *Sci. Robot.*, vol. 5, no. 41, Apr. 2020, Art. no. eaaz 4239.
- [19] M. Boyvat, D. M. Vogt, and R. J. Wood, "Ultrastrong and high-stroke wireless soft actuators through liquid-gas phase change," *Adv. Mater. Technol.*, vol. 4, no. 2, Feb. 2019, Art. no. 1800381.
- [20] V. Cacucciolo, J. Shintake, Y. Kuwajima, S. Maeda, D. Floreano, and H. Shea, "Stretchable pumps for soft machines," *Nature*, vol. 572, no. 7770, pp. 516–519, Aug. 2019.
- [21] 3M Company, "3M novoc 7000 engineered fluid." Nov. 2020. [Online]. Available: <https://multimedia.3m.com/mws/media/1213720/3m-novoc-7000-engineered-fl%uid-tds.pdf>
- [22] E. S. Chan, T. K. Lim, W. P. Voo, R. Pogaku, B. T. Tey, and Z. Zhang, "Effect of formulation of alginate beads on their mechanical behavior and stiffness," *Particuology*, vol. 9, no. 3, pp. 228–234, Jun. 2011.
- [23] Y. Gu, H. Kojima, and N. Miki, "Theoretical analysis of 3D emulsion droplet generation by a device using coaxial glass tubes," in *Sensors Actuators, A: Phys.*, vol. 169, no. 2, Oct. 2011, pp. 326–332.
- [24] H. Yasuga, K. Kamiya, S. Takeuchi, and N. Miki, "Self-Generation of two-dimensional droplet array using oil-water immiscibility and replacement," *Lab Chip*, vol. 18, no. 7, pp. 1130–1137, Apr. 2018.
- [25] T. Usui, H. Ishizuka, T. Hiraki, Y. Kawahara, S. Ikeda, and O. Oshiro, "Miniaturized liquid pouch motors using flexible liquid metal heater," in *Proc. 33rd Int. Microprocesses Nanotechnol. Conf.*, 2020, pp. 1–2.
- [26] F. Meder, G. A. Naselli, A. Sadeghi, and B. Mazzolai, "Remotely light-powered soft fluidic actuators based on plasmonic-driven phase transitions in elastic constraint," *Adv. Mater.*, vol. 31, no. 51, Dec. 2019, Art. no. 1905671.
- [27] T. Hiraki *et al.*, "Laser pouch motors: Selective and wireless activation of soft actuators by laser-powered liquid-to-gas phase change," *IEEE Robot. Automat. Lett.*, vol. 5, no. 3, pp. 4180–4187, Jul. 2020.
- [28] S. Ueno and Y. Monnai, "Wireless soft actuator based on liquid-gas phase transition controlled by millimeter-wave irradiation," *IEEE Robot. Automat. Lett.*, vol. 5, no. 4, pp. 6483–6488, Oct. 2020.
- [29] S. Sawano, K. Naka, A. Werber, H. Zappe, and S. Konishi, "Sealing method of pdms as elastic material for mems," in *Proc. 21st IEEE Int. Conf. Micro Electron. Mech. Syst.*, 2008, pp. 419–422.